

EWI-2 negatively regulates TGF- β signaling leading to altered melanoma growth and metastasis

Hong-Xing Wang¹, Chandan Sharma¹, Konstantin Knoblich¹, Scott R Granter², Martin E Hemler¹

¹Department of Cancer Immunology and AIDS, Dana-Farber Cancer Institute and Department of Pathology, Harvard Medical School, Boston, MA 02215, USA; ²Department of pathology, Brigham and Women's Hospital, Boston, MA 02215, USA

In normal melanocytes, TGF- β signaling has a cytostatic effect. However, in primary melanoma cells, TGF- β -induced cytostasis is diminished, thus allowing melanoma growth. Later, a second phase of TGF- β signaling supports melanoma EMT-like changes, invasion and metastasis. In parallel with these “present-absent-present” TGF- β signaling phases, cell surface protein EWI motif-containing protein 2 (EWI-2 or IgSF8) is “absent-present-absent” in melanocytes, primary melanoma, and metastatic melanoma, respectively, suggesting that EWI-2 may serve as a negative regulator of TGF- β signaling. Using melanoma cell lines and melanoma short-term cultures, we performed RNAi and overexpression experiments and found that EWI-2 negatively regulates TGF- β signaling and its downstream events including cytostasis (*in vitro* and *in vivo*), EMT-like changes, cell migration, CD271-dependent invasion, and lung metastasis (*in vivo*). When EWI-2 is present, it associates with cell surface tetraspanin proteins CD9 and CD81 — molecules not previously linked to TGF- β signaling. Indeed, when associated with EWI-2, CD9 and CD81 are sequestered and have no impact on T β R2-T β R1 association or TGF- β signaling. However, when EWI-2 is knocked down, CD9 and CD81 become available to provide critical support for T β R2-T β R1 association, thus markedly elevating TGF- β signaling. Consequently, all of those TGF- β -dependent functions specifically arising due to EWI-2 depletion are reversed by blocking or depleting cell surface tetraspanin proteins CD9 or CD81. These results provide new insights into regulation of TGF- β signaling in melanoma, uncover new roles for tetraspanins CD9 and CD81, and strongly suggest that EWI-2 could serve as a favorable prognosis indicator for melanoma patients.

Keywords: melanoma; EWI-2/IgSF8; TGF- β 1; tetraspanins; CD9; CD81

Cell Research (2015) 25:370-385. doi:10.1038/cr.2015.17; published online 6 February 2015

Introduction

Malignant melanoma, a form of skin cancer arising from malignantly transformed melanocytes, is one of the most aggressive and drug-resistant human cancers [1, 2]. With its considerable metastatic potential, melanoma accounts for over 70% of skin cancer-related deaths [1, 3]. Transforming growth factor- β (TGF- β) plays a key role during melanoma progression. In normal melanocytes, TGF- β exerts a potent anti-proliferative effect. However, in primary melanoma, sensitivity to TGF- β is diminished, and thus cell growth is facilitated. After that,

TGF- β signaling reappears, in support of melanoma epithelial-mesenchymal-transition (EMT) and metastasis [4-6]. At present, efforts are underway to understand how changes in TGF- β sensitivity are regulated and to develop strategies for inhibiting TGF- β -dependent melanoma progression and metastasis.

Here we demonstrate that changes in the expression level of EWI motif-containing protein 2 (EWI-2, or IgSF8/CD316), a cell surface transmembrane protein, play a key role in orchestrating critical shifts in TGF- β signaling phases (“present-absent-present”). EWI-2 is a member of an Ig subfamily that comprises proteins with a conserved Glu-Trp-Ile (EWI) motif [7]. EWI-2 associates directly with tetraspanins CD9 and CD81 on the cell surface [7-9], and functions to alter their molecular organization [10, 11]. While CD9 and CD81 have been suggested to contribute to melanoma invasion and/or transendothelial migration [12-14], other studies have

Correspondence: Martin E Hemler

Tel: +44-617-632-3410; Fax: +44-617-632-2662

E-mail: martin_hemler@dfci.harvard.edu

Received 14 May 2014; revised 24 September 2014; accepted 7 November 2014; published online 6 February 2015

revealed an inverse correlation between CD9 levels and melanoma invasion/metastasis [15, 16]. Neither CD9 nor CD81 has been previously linked to TGF- β signaling.

Although specific molecular functions of EWI-2 are currently unknown, EWI-2 has been reported to negatively regulate cell spreading, motility, invasion, and filopodia formation [10, 17, 18]. Also EWI-2 may play a role during cell infection by hepatitis C virus (HCV) [19] and during sperm-oocyte fusion [20]. An elevated EWI-2 expression level leads to diminished glioblastoma growth [18] and is associated with increased survival in human glioma patients [18]. However, EWI-2 has not been previously linked functionally to either melanoma or TGF- β signaling.

To evaluate the role of EWI-2 in melanoma, we analyzed melanoma patient samples, human and mouse melanoma cell lines, and a panel of primary melanoma short-term cultures (MSTCs) [21] with variable EWI-2 levels. *In vivo* and *in vitro* analyses coupled with knockdown and overexpression of EWI-2 revealed that EWI-2 negatively regulates TGF- β signaling, thus explaining the paradoxical roles of EWI-2 in melanoma, i.e., support of melanoma growth/proliferation, but inhibition of invasion/metastasis. Furthermore, we uncovered novel roles for tetraspanins CD9 and CD81. These proteins make no contributions to TGF- β signaling in melanoma cells when EWI-2 is present. However, the upregulated TGF- β -dependent functions that specifically arise due to knockdown of EWI-2 are almost entirely dependent on tetraspanin proteins CD9 and CD81. Taken together, these results (i) provide new insights into the anti-proliferative, pro-invasion, and pro-metastasis effects of TGF- β signaling in melanocytes and melanoma cells [4, 6, 22], (ii) suggest that therapeutic targeting of CD9 and/or CD81 may effectively diminish TGF- β signaling during progression and metastasis of EWI-2^{Low} melanomas, and perhaps other EWI-2^{Low} cancers, and (iii) suggest that elevated EWI-2 expression levels would predict favorable melanoma patient outcomes.

Results

EWI-2 expression in melanoma samples

Previous studies revealed that EWI-2 gene expression was significantly elevated in human melanoma cell lines, compared to other tumor cell types [23]. To confirm and extend those results, we carried out immunohistochemical analyses of the EWI-2 protein. EWI-2 is minimally expressed in normal skin melanocytes, normal skin tissues, or benign nevi (Figure 1A-1C). However, staining signals were elevated significantly in primary melanoma, and to a lesser extent in human metastatic melanoma

samples (Figure 1B, 1C and Supplementary information, Figure S1A). EWI-2 levels were also significantly elevated in pigmented melanomas (60.6% with a score of ≥ 4) and in acral lentiginous melanomas (55.6% with a score of ≥ 4 ; data not shown).

EWI-2 negatively regulates metastasis and invasion of melanoma

EWI-2 was abundantly expressed in the majority of 11 MSTCs (Supplementary information, Figure S1B, top). Those MSTCs expressing the highest levels of EWI-2 were the least active in trans-Matrigel invasion (Figure 1D), suggesting that EWI-2 could inhibit invasion. Indeed, stable knockdown of EWI-2 in human SK-Mel-28 and mouse B16F10 melanoma cell lines significantly increased both cell migration and invasion (Figure 2A). Similar results were obtained upon transient depletion of EWI-2 (Figure 2B). Conversely, EWI-2 overexpression inhibited cell invasion in two MSTCs (Figure 2C).

We next investigated the effects of EWI-2 depletion on tumor metastasis in mouse models that received intravenous (i.v.) injection of melanoma cells. Consistent with the above results, stable knockdown of EWI-2 in human SK-Mel-28 and mouse B16F10 cell lines, in each case using two different shRNAs, resulted in a significant increase in metastatic lung colony numbers after 6 weeks and 16 days, respectively (Figure 2D and 2E). Sizes of metastatic colonies were not increased, but rather were slightly decreased (Figure 2D and 2E, lower right panels). Thus, EWI-2 likely inhibits human and mouse melanoma cell metastasis by inhibiting tissue invasion rather than colony growth.

We also tested the effect of EWI-2 knockdown in another mouse model, in which SK-Mel-28 cells were subcutaneously (s.c.) injected into nude mice. At the s.c. injection sites of primary SK-Mel-28 tumor growth in nude mice receiving control or EWI-F-depleted cells, tumor borders were invariably smooth (Supplementary information, Figure S2). EWI-F, which belongs to the “EWI” subfamily and is 27% identical to EWI-2 [7, 24], serves here as a useful negative control. By contrast, EWI-2-knockdown tumors, in 2 out of 4 samples examined, yielded irregular borders, consistent with enhanced invasion (Supplementary information, Figure S2). Knockdown efficiencies of EWI-2 and EWI-F are demonstrated in Supplementary information, Figure S3A-S3E.

EWI-2 depletion also markedly affected intrinsic cell morphology, again consistent with enhanced invasion and metastasis. Control SK-Mel-28 cells were polygonal with a few short branches. By contrast, EWI-2-depleted cells were more elongated, showing a significantly increased ‘deviation from round’ (Supplementary informa-

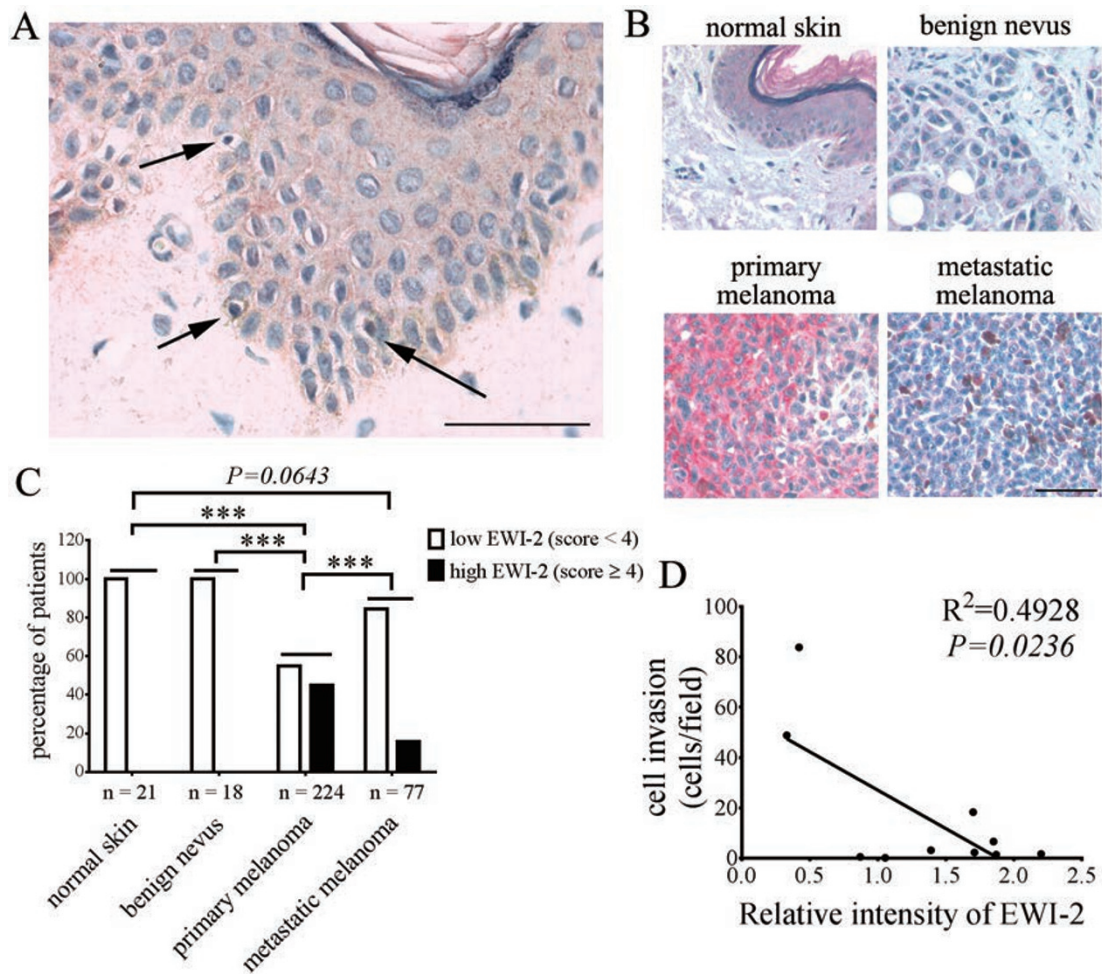


Figure 1 Elevated EW1-2 expression levels in melanoma samples. **(A)** Normal skin melanocytes (arrows) showed no EW1-2 staining as indicated in a representative panel and in 16 other normal skin sections (data not shown). **(B)** EW1-2 protein detected in tissue sections from the indicated sources. **(C)** For statistical analyses, tissue samples are subdivided into 'high' (score ≥ 4) and 'low' (score < 4) categories according to EW1-2 levels. P values are from Fisher's exact test. $***P < 0.001$. EW1-2 expression level in metastatic samples was not significantly higher than that in either normal skin or benign nevi, but was significantly higher than that in combined normal skin and benign nevus samples ($P < 0.01$). Supplementary information, Figure S1A shows representative images to demonstrate EW1-2 scoring. **(D)** EW1-2 levels measured by western blot assays (relative to GAPDH; $n = 5$ for each point) in MSTCs correlate negatively with invasive potential ($n = 4$ for each point).

tion, Figure S4A). EW1-2-depleted cells also showed significantly enhanced elongation and cable formation when plated on Matrigel (Supplementary information, Figure S4B). Decreased cell-cell adhesion often accompanies cell invasion [25]. In EW1-2-depleted SK-Mel-28 cells, cell-cell clustering was significantly decreased relative to control cells (Supplementary information, Figure S4C), and adherence junction proteins β -catenin and E-cadherin were diminished (Supplementary information, Figure S4D). Immunostaining confirmed diminished β -catenin expression at the membrane and nucleus (data not shown). These changes, together with increased vimentin

expression (Supplementary information, Figure S4D), are consistent with enhanced EMT in EW1-2-knockdown cells.

EW1-2 supports melanoma cell growth in vivo and in vitro

To analyze *in vivo* effects of EW1-2 on primary melanoma cell growth, we injected SK-Mel-28 cells (EW1-2-depleted, EW1-F-depleted, or vector control) subcutaneously into the flanks of nude mice. After 10 days, tumors appeared at the inoculation sites of most mice injected with vector control and EW1-F-knockdown cells ($\sim 90\%$), but were visible in only $\sim 50\%$ of mice in-

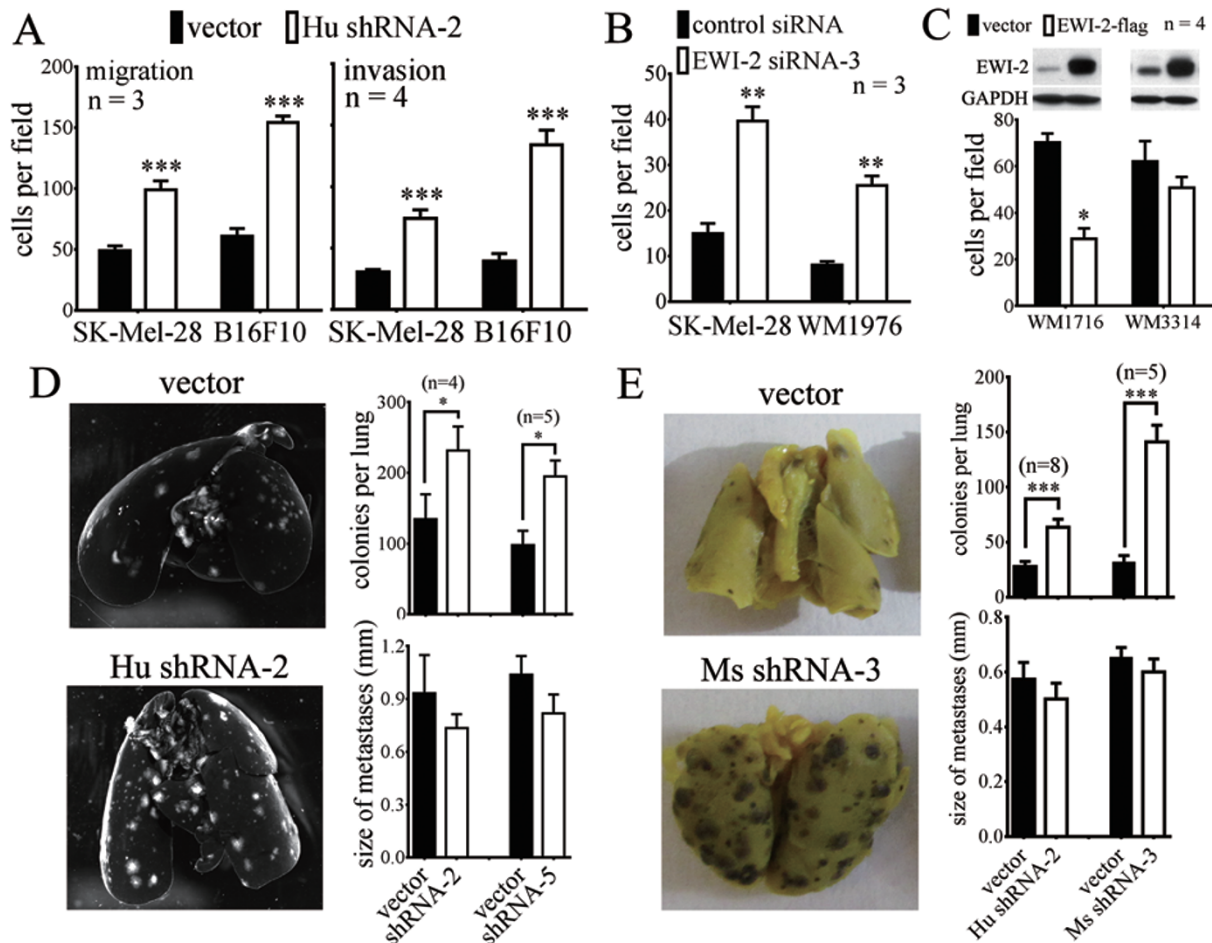


Figure 2 EWI-2 inhibits migration, invasion and metastasis of melanoma. **(A)** Stably depleted SK-Mel-28 and B16F10 cells were tested for migration and invasion. Mean cell number values represent results from different wells. Within each well, 10 different fields were measured. The data are presented as mean \pm SE in this and all following graphs unless otherwise indicated. **(B)** Transiently depleted SK-Mel-28 and MSTC WM1976 were tested for invasion. **(C)** Two different MSTCs with or without EWI-2 overexpression were tested for cell invasion. **(D, E)** Stable EWI-2 knockdown elevated lung metastasis for human SK-Mel-28 **(D)** and mouse B16F10 **(E)** cells. Tumor colonies on surfaces of each lobe were counted, and 2D diameters were measured and used for statistical analysis. * $P < 0.05$; ** $P < 0.01$; *** $P < 0.001$. Knockdown efficiencies are indicated in Supplementary information, Figure S3.

jected with EWI-2-depleted cells (Figure 3A). Tumor appearance was significantly delayed upon EWI-2 knockdown ($P = 0.02$, Figure 3A), and tumors also showed significantly reduced volume (Figure 3B) and weight (after 49 days; Figure 3C). By contrast, depletion of EWI-F did not affect tumor incidence, volume or weight (Figure 3A-3C). Similar results were obtained in two additional experiments (data not shown). Thus, EWI-2 (but not EWI-F) supports SK-Mel-28 cell xenograft growth.

Stable EWI-2 depletion, but not EWI-F depletion, also significantly diminished tumor cell growth *in vitro* in SK-Mel-28 (Figure 3D), SK-Mel-5, 501mel and B16F10 cell lines (Supplementary information, Figure S5A), as de-

termined by cell counting. Consistent with these results, EWI-2 expression levels in a group of 11 MSTCs positively correlated with cell proliferation (Figure 3E). In accord with EWI-2 shRNA results, four different EWI-2 siRNAs with comparable knockdown potency (Supplementary information, Figure S3C) also significantly impaired proliferation of representative MSTCs (WM1862 and WM1976) and SK-Mel-28 cells (Supplementary information, Figure S5B). EWI-2-depleted melanoma cells also showed significantly diminished cell growth in an MTT cell proliferation assay (data not shown). In further experiments, EWI-2 depletion decreased the percentage of SK-Mel-28 cells in G2/M phases (36.7 \rightarrow 18.2%), with

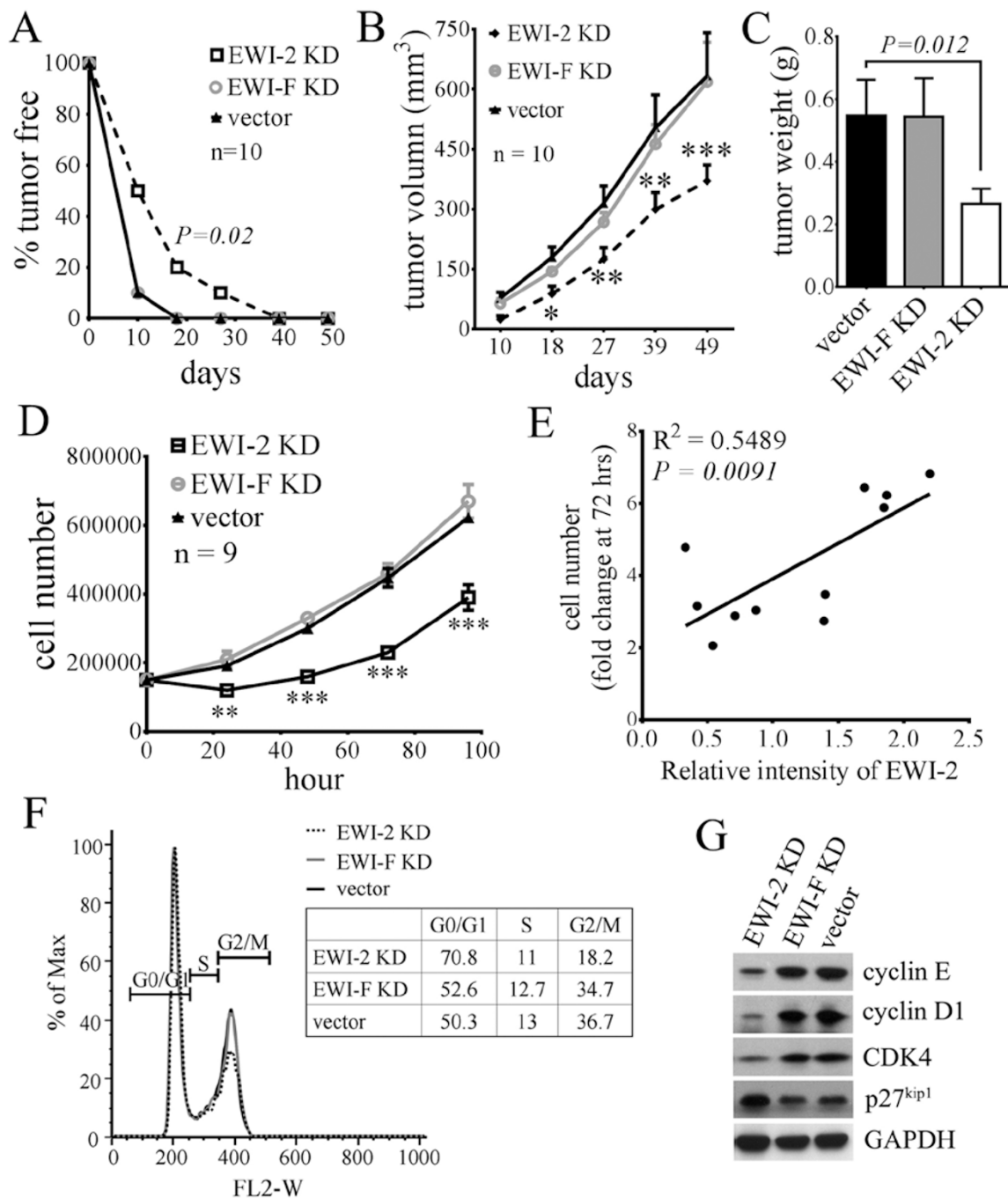


Figure 3 EWI-2 supports primary tumor xenograft growth. **(A-C)** Control, EWI-2-knockdown (KD) or EWI-F-KD SK-Mel-28 cells were subcutaneously injected into nude mice. **(A)** EWI-2 KD in SK-Mel-28 cells delays tumor appearance. P is from the log rank test. **(B)** EWI-2 KD (but not EWI-F KD) reduces tumor volume. Tumor size was measured every 5-7 days and volumes were calculated as length \times width² \times 0.52. Differences between EWI-2-KD and control cells are significant, $*P < 0.05$; $**P < 0.01$; $***P < 0.001$. **(C)** EWI-2 KD reduces tumor weight. At the termination of the study (50 days), tumors were excised from each mouse and weighed ($n = 10$ for each group). **(D)** EWI-2 depletion diminishes cell expansion in cultured SK-Mel-28 cells, as revealed by cell counting. $**P < 0.01$; $***P < 0.001$. **(E)** EWI-2 expression levels in MSTCs positively correlate with cell proliferation ($n = 4$ for each point). **(F)** EWI-2 depletion induces cell cycle arrest, as determined by flow cytometric analysis of propidium iodide-stained SK-Mel-28 cells. Results from multiple experiments showed that the percentage of cells in the G2/M phase was significantly lower in EWI-2-KD cells, compared with vector and EWI-F-KD cells ($P < 0.01$). Almost identical results were obtained using MSTCs WM1862 and WM1976 (mentioned in the text). **(G)** EWI-2 depletion affects expression of key cell cycle regulatory proteins, as indicated by immunoblotting.

a corresponding increase in G0/G1 phases (Figure 3F). Similar cell cycle changes were seen when EWI-2 was knocked down in MSTCs WM1862 (G2/M, 36.5% → 17.3%) and WM1976 (G2/M, 36.4% → 20.1%; Supplementary information, Figure S5C). Also, expression levels of key cell cycle proteins (cyclin E, cyclin D1, and CDK4) were decreased by 59%-82%, while expression level of the cell cycle inhibitor p27^{kip1} was increased by 2.1-fold (Figure 3G). By contrast, depletion of EWI-F did not affect cell cycle progression or the expression of cell cycle regulatory proteins (Figure 3F and 3G).

DNA array evidence for increased TGF-β signaling upon EWI-2 depletion

Gene microarray analysis yielded unbiased insight into the paradoxical effects of EWI-2 on melanoma metastasis/invasion and tumor growth. In EWI-2-depleted SK-Mel-28 cells, 471 genes were upregulated and 528 genes were downregulated (> 2-fold change; $P < 0.05$; Supplementary information, Figure S6A and Table S1). Potential upstream regulators responsible for these gene expression changes were then ranked in order of significance, using the Ingenuity Pathway ‘Core Analysis’ function. TGF-β1 appeared in position 2 (Supplementary information, Figure S6B, $P = 7.74E-23$). TGF-β signaling has been well established to inhibit melanoma cell growth and to support melanoma metastasis [4-6]. Other potential upstream regulators listed in Supplementary information, Figure S6B (TP53, MYC, CDKN1A, VEGF, HGF) were not considered further because (i) some of them showed only minimal expression in SK-Mel-28 cells regardless of EWI-2 expression (TP53, MYC, and CDKN1A), (ii) activation of some of these genes (TP53 and CDKN1A) is not consistent with the increased invasion and migration observed upon EWI-2 depletion, and (iii) inhibition of some of these genes (MYC, VEGF, and HGF) cannot explain both the diminished proliferation/survival and increased invasion/migration observed in EWI-2-depleted cells.

EWI-2 negatively regulates TGF-β1 signaling

Supplementary information, Table S2 lists 10 genes (taken from Supplementary information, Table S1) that are (i) upregulated upon EWI-2 depletion, (ii) known to be TGFβ-inducible, and (iii) directly dependent on Smad2/3 (a downstream mediator of canonical TGFβ signaling) for transcriptional activation [26-29]. Furthermore, depletion of EWI-2 in SK-Mel-28 cells (not serum-starved) markedly enhanced basal phosphorylation of Smad2 (Figure 4A), which is indicative of enhanced endogenous TGF-β signaling. EWI-2 depletion did not change the level of endogenous TGF-β1 protein in

whole-cell lysates (Figure 4B, lanes 1, 2) or in cell culture media (Figure 4B, lanes 3, 4). Likewise, EWI-2 depletion did not change the activity of TGF-β1 produced by SK-Mel-28 cells, as seen in a standard biochemical assay (data not shown). Therefore, we hypothesized that EWI-2 depletion might change cell sensitivity to TGF-β. Indeed, EWI-2 depletion markedly increased the sensitivity of serum-starved cells to exogenously added latent (Figure 4C) or active TGF-β1 (Supplementary information, Figure S6D). Compared to control cells, EWI-2-depleted cells showed 5.6- and 4.9-fold elevation of Smad2 phosphorylation after treatment with 10 ng/ml and 50 ng/ml latent TGF-β1, respectively (Figure 4C). It is noteworthy that cells used in Figure 4C and Supplementary information, S6D were serum-starved, and thus showed little background/basal TGF-β signaling activity (in contrast to results shown in Figure 4A). An inhibitor of the TGF-β type I receptor (TβR1) kinase activity (SB-431542) [30] completely abrogated TGFβ1-stimulated phosphorylation of Smad2 (Figure 4C). Furthermore, moderate phospho-Smad2/3 (p-Smad2/3) staining was observed in nuclei of EWI-2-depleted, non-serum-starved cells, but not in vector control cells (Figure 4D, top panels). This difference was even more obvious after treatment with 50 ng/ml latent TGF-β1 (Figure 4D, middle panels). Nuclear accumulation of p-Smad2/3 was completely blocked by SB-431542 (Figure 4D, bottom panels). Enhanced TGF-β signaling upon EWI-2 knockdown was also observed *in vivo*. Staining of SK-Mel-28 tumor xenograft tissue sections showed significantly upregulated Smad2/3 phosphorylation in tumors derived from EWI-2-depleted cells (Figure 4E). Further evidence for an inverse relationship between EWI-2 and pSmad2/3 levels was seen in human patient tissue samples. Those with the lowest EWI-2 levels showed the most elevated levels of p-Smad2/3 staining (Figure 4F and 4G). In further support of EWI-2 as a negative regulator of TGF-β signaling, EWI-2 overexpression in two MSTCs (WM1716 and WM3314) decreased Smad2 activation (by 55% and 11%, respectively; Figure 4H).

TGF-β signaling is almost entirely responsible for altered invasion and proliferation in EWI-2-depleted melanoma cells

We hypothesized that enhanced TGF-β signaling seen in EWI-2-depleted melanoma cells would explain the altered cell invasion and proliferation. Indeed, in SK-Mel-28 cells treated with SB-431542, EWI-2 knockdown showed less inhibitory effects on levels of cyclin D1 and CDK4, involved in cell cycle progression (Figure 5A, compare lanes 1, 2 with 3, 4). Also, in SK-Mel-28 cells treated with SB-431542 or Smad2 siRNA, EWI-2 deple-

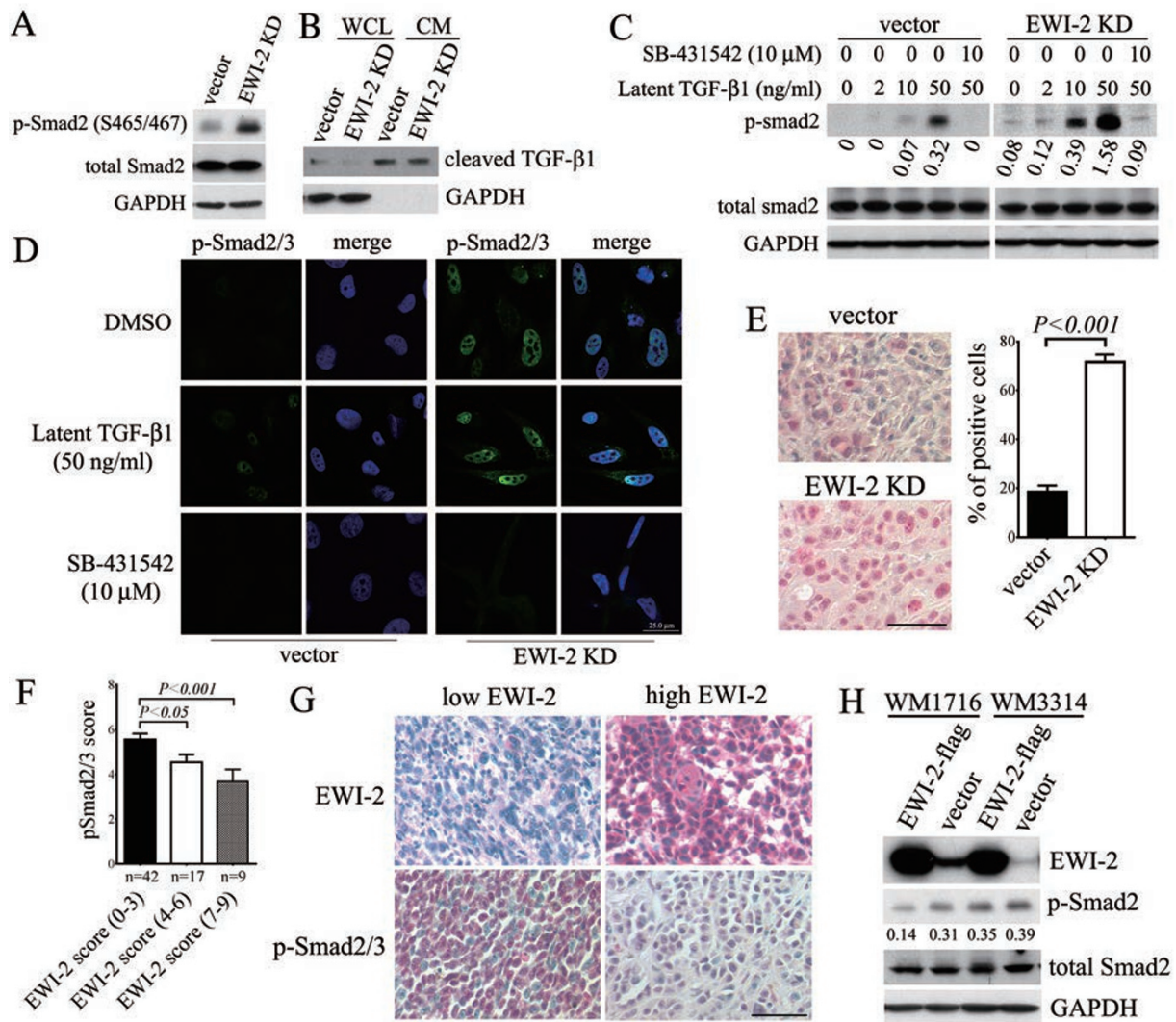


Figure 4 EWI-2 negatively regulates TGF-β1 signaling. **(A)** EWI-2 depletion stimulates Smad2 phosphorylation, without changing total Smad2 levels. SK-Mel-28 cells were cultured in complete medium for 48 h. **(B)** EWI-2 depletion did not affect TGF-β1 secretion. SK-Mel-28 cells were cultured in serum-free medium for 24 h, and then the culture medium was collected, concentrated and analyzed by SDS-PAGE (lanes 3, 4). Also whole-cell lysates (from 1% Trion X-100 lysis buffer) were analyzed (lanes 1, 2). The observed size of cleaved TGF-β1 is ~12 kDa. **(C)** EWI-2 knockdown enhances cell sensitivity to TGF-β1. Cells were starved for 6 h prior to treatment with the indicated concentrations of latent human TGF-β1 and SB-431542 (a specific inhibitor of TβR1 kinase activity). Numbers represent phospho/total Smad2 ratios. **(D)** Immunofluorescence of p-Smad2/3 after the indicated treatments. **(E)** Representative mouse xenograft sections were stained for p-Smad2/3 (red) and nuclei were counterstained (blue). The percentage of p-Smad2/3-positive cells was quantitated using Image J software. **(F)** Human tissue microarray sections (ME1004a) were stained for EWI-2 and p-Smad2/3, with scoring as mentioned in Supplementary information, Figure S1A. Mean p-Smad2/3 scores are shown for subsets of samples having various EWI-2 scoring as indicated. Samples include malignant primary and metastatic melanomas. **(G)** Representative images of p-Smad2/3 staining in the low-EWI-2 (sample no. G7) and high-EWI-2 (sample no. F5) samples. **(H)** EWI-2 overexpression inhibits Smad2 activation. Numbers represent phospho/total Smad2 ratios.

tion no longer caused cell cycle arrest or inhibited cell proliferation (Figure 5B and Supplementary information, Figure S7A and S7B). Conversely, effects of EWI-2 depletion were accentuated in the presence of added latent TGF-β1, as cyclin D1 and CDK4 essentially disappeared

under such conditions (Figure 5A, compare lanes 3, 4 with 5, 6).

TGF-β1-triggered EMT, which leads to increased invasion and metastasis and decreased cell-cell adhesion, is typically accompanied by downregulation of adher-

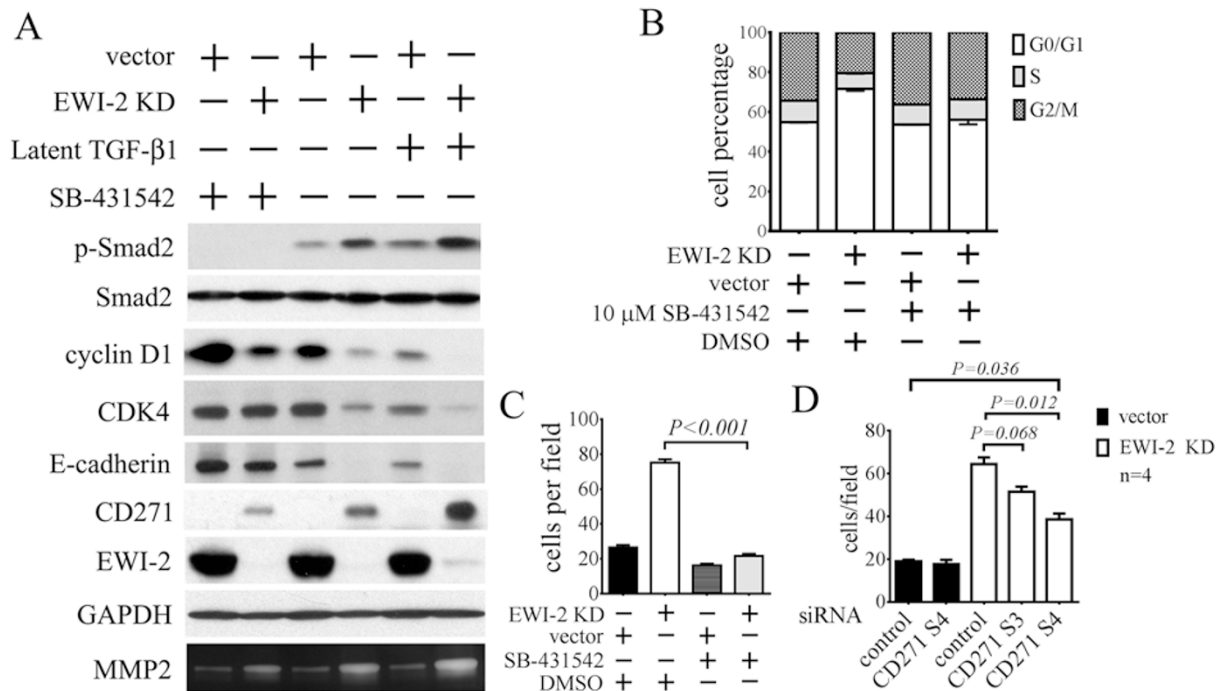


Figure 5 Inhibition of TGF- β 1 signaling reverses effects of EWI-2 depletion. **(A)** SK-Mel-28 cells, with or without EWI-2 depletion, were treated with 10 μ M SB-431542 for 16 h or 20 ng/ml latent TGF- β 1 for 24 h. Cell lysates were then blotted for the indicated proteins. MMP2 activity, in serum-free medium at 48 h, was examined by gelatin zymography. **(B)** Treatment of SK-Mel-28 cells with SB-431542 diminished effects of EWI-2 depletion on cell cycle progression. SK-Mel-28 cells were treated with 10 μ M SB-431542 or the same volume of DMSO for 16 h, and then fixed in 70% ethanol for cell cycle analysis as described in Materials and Methods. Results from multiple experiments showed that 10 μ M SB-431542 completely rescued the changes in cell percentages in G0/G1 and G2/M phases in EWI-2-KD cells, compared with vector cells ($P > 0.05$). **(C)** SK-Mel-28 cells, with or without EWI-2 depletion, were tested for cell invasion in the presence of 10 μ M SB-431542 or the same volume of DMSO following the standard protocol. For each condition, $n = 6$. **(D)** SK-Mel-28 cells (control or depleted for EWI-2) were also treated with CD271 siRNA #4, or CD271 siRNA #3 or control siRNA (knockdown efficiency was validated in Supplementary information, Figure S3F) and then cell invasion was measured.

ins junction protein E-cadherin [31], and can lead to upregulation of metastasis-associated proteins such as MMP2 [32, 33]. Indeed, when cells were treated with SB-431542, EWI-2 depletion no longer stimulated cell invasion (Figure 5C), or downregulated E-cadherin expression (Figure 5A, compare lanes 1, 2 with 3, 4). Also, levels of MMP2 and CD271/NGFR (another molecule linked to melanoma metastasis [33, 34]) were not increased to the same extent. Conversely, effects of EWI-2 depletion on CD271 and MMP2 production were markedly enhanced when latent TGF- β 1 was added (Figure 5A, compare lanes 3, 4 with 5, 6), consistent with increased cell sensitivity to TGF- β 1 upon EWI-2 knockdown. In a control experiment, invasion inhibited by 2 μ M SB-431542 was almost completely reversed by addition of excess latent TGF- β 1 (Supplementary information, Figure S8). Hence, effects of SB-431542 on invasion are largely due to inhibition of TGF- β signaling.

Moreover, Smad2 knockdown significantly blocked the elevated invasion capacity of EWI-2-depleted cells (Supplementary information, Figure S7C). However, EWI-2 depletion in SK-Mel-28 cells did not enhance activation of FAK, Erk1/2, or Akt (Supplementary information, Figure S7D), even though these molecules can sometimes be activated by TGF- β 1 [35, 36]. Together these results show that the canonical TGF- β 1 signaling pathway (i.e., through Smad2/3) plays a dominant role in EWI-2-mediated regulation of melanoma cell cycle progression, EMT, and invasion.

The *CD271/NGFR* gene was the third highest among all genes upregulated due to EWI-2 depletion (Supplementary information, Table S1, bottom). Transient knockdown of CD271 had no effect on background invasion. However, CD271 knockdown partially reversed the stimulation of invasion caused by EWI-2 depletion (Figure 5D), with the reversal effects (Figure 5D) propor-

tional to CD271 knockdown efficiencies (Supplementary information, Figure S3F). Control siRNA had no effect on either CD271 expression (Supplementary information, Figure S3F) or invasion (Figure 5D). These results establish that CD271, a molecule previously linked to melanoma metastasis [33, 34], is a major contributor to the TGF β -dependent invasion that is facilitated by EWI-2 depletion.

EWI-2 indirectly affects T β R1-T β R2 association: critical roles for tetraspanin proteins CD9 and CD81

To gain mechanistic insight into enhanced TGF- β 1 signaling upon EWI-2 depletion, we analyzed the formation of T β R1-T β R2 receptor complexes, which play a critical role in TGF- β signaling initiation [26-29]. Upon EWI-2 depletion, the amount of T β R1 co-immunoprecipitated with T β R2 increased by > 4-fold (Figure 6A). Expression levels of total T β R2 and T β R1, and cell surface T β R2 and T β R1 were only minimally changed (Supplementary information, Figure S6C). Immunoprecipitation of EWI-2 did not yield any associated T β R1 or T β R2 (data not shown), suggesting that EWI-2 acts indirectly.

How does EWI-2 indirectly regulate T β R2-T β R1 association? To address this issue we focused on tetraspanin proteins CD9 and CD81, which are the major protein partners for EWI-2 in multiple cell types [7-9]. Consistent with previous reports, EWI-2 in SK-Mel-28 cells associated with tetraspanin proteins CD9 and CD81, but not with CD151, as shown by co-immunoprecipitation

(Supplementary information, Figure S9A). CD151 serves as a useful negative control as it is a relatively abundant tetraspanin, but does not associate with EWI-2 [7-9]. The amounts of EWI-2 recovered from CD9 and CD81 immunoprecipitates (82% and 78%, Supplementary information, Figure S9A, lanes 2 and 3, lower panel) are comparable to the amounts directly immunoprecipitated, suggesting that nearly all EWI-2 present are associated with CD9 and CD81 (Supplementary information, Figure S9A). It was previously suggested that EWI-2 association shifts CD9 from homoclusters, detected using anti-CD9 mAb C9BB, to heteroclusters, which show diminished recognition by mAb C9BB [11]. Consistent with this, depletion of EWI-2 from melanoma cells caused a substantial increase in the fraction of oligomerized CD9 (from ~40% to ~70%) detected by mAb C9BB, relative to total CD9 (detected using CD9 mAb MM2/57; Supplementary information, Figure S9B).

Because EWI-2 depletion enhances T β R1-T β R2 association (Figure 6A) and causes a marked oligomerization of CD9 (Supplementary information, Figure S9B), we tested whether CD9 might contribute to T β R1-T β R2 association. Indeed, the substantial increase in T β R1-T β R2 association upon EWI-2 depletion (Figure 6B, lanes 7 and 8) was almost completely reversed by knockdown of either CD9 or CD81, but not CD151 (Figure 6B, lanes 1-6). Notably, CD9 and CD81 knockdown had minimal effect on background levels of T β R1-T β R2 association seen in the presence of EWI-2 (Figure 6B, dark bars).

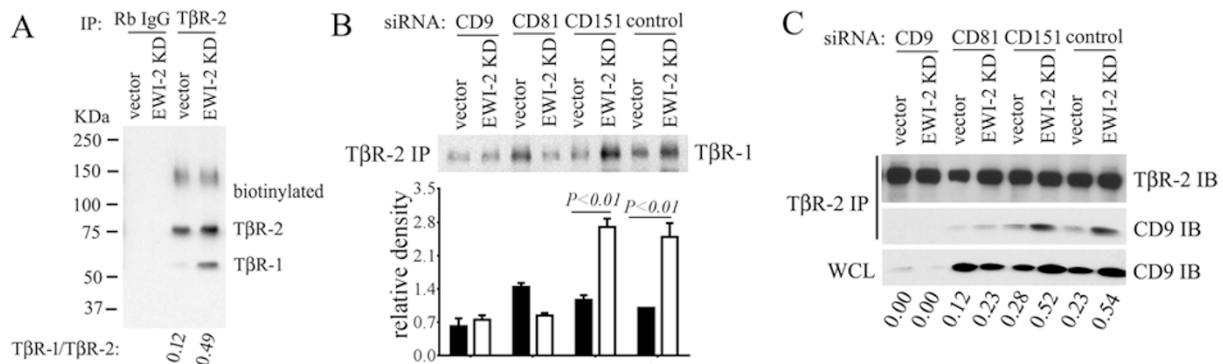


Figure 6 Depletion of EWI-2 changes the formation of the T β R1/T β R2 complex. **(A)** EWI-2 depletion increases the interaction of T β R2 and T β R1. Cells were labeled with biotin, lysed in Brij 96 lysis buffer, and then after preclearing, anti-T β R2 antibody was used for immunoprecipitation. Bands were developed after ExtrAvidin incubation and enhanced chemiluminescence (ECL) detection. Numbers represent T β R1/T β R2 ratios. Rabbit IgG was used as a negative control. **(B)** Effects of EWI-2 and tetraspanin protein knockdown on T β R2-T β R1 interaction. After siRNA treatment (72 h), cells were incubated with latent TGF- β 1 (20 ng/ml; 30 min), lysed in 1% Brij 99 lysis buffer, and then T β R2 was immunoprecipitated. The eluted samples were then blotted for T β R1. Quantitation is shown in the lower panel ($n = 4$). **(C)** T β R2 interacts with CD9 in EWI-2-depleted cells. Eluted samples from **B** were blotted for T β R2, EWI-2, CD9, CD81, and CD151, but only the T β R2 and CD9 bands were observed. Numbers represent the ratio of CD9 in T β R2 immunoprecipitated samples to CD9 in WCL. Efficiency of CD9 knockdown and presence of CD9 in whole cell lysates was confirmed in Supplementary information, Figure S9C.

Further implicating CD9, co-immunoprecipitation of T β R2 with CD9 (Figure 6C; lanes 7 and 8, middle panel) was markedly enhanced by knockdown of EWI-2. Increased CD9-T β R2 interaction caused by EWI-2 depletion was prevented by knockdown of CD81 (lanes 3 and 4, middle panel), but not by knockdown of CD151 (lanes 5 and 6, middle panel). Hence, CD81 contributes to CD9-T β R2 association, which helps to explain CD81 contributions to CD9-dependent T β R1-T β R2 association. Levels of immunoprecipitated T β R2 in all samples (Figure 6C, lanes 1-8, top panel) and CD9 in whole cell lysates (Figure 6C, lanes 3-8, lower panel) were minimally changed. Other control experiments (Supplementary information, Figure S9C) confirmed the specificity and > 95% effectiveness of all knockdowns, and showed that the expression levels of T β R2 and T β R1 proteins were minimally affected by removal of CD9, CD81, or CD151.

If CD9 and CD81 support T β R1-T β R2 association in EWI-2-depleted cells, they should also support TGF- β -dependent signaling in these cells. Indeed, the 2-3-fold increase in Smad2 phosphorylation caused by EWI-2 depletion (Figure 7A, lanes 7 and 8), was abolished by knockdown of CD9 or CD81, but not CD151 (Figure 7A, lanes 1-6). Furthermore, increased Smad2 phosphorylation in EWI-2-depleted cells was significantly reversed by treatment of intact cells with 2 different anti-CD9 mAbs (C9BB and MM2/57) and to a lesser extent by an anti-CD81 mAb (Figure 7B). Notably, CD9 and CD81 siRNAs and anti-CD9, anti-CD81 antibodies had minimal effect on p-Smad2 when EWI-2 was present (Figure 7A and 7B, dark bars).

Given that TGF- β 1 signaling is responsible for the diminished cell proliferation and enhanced invasion of EWI-2-depleted cells (Figure 5B and 5C), and that tetraspanins CD9 and CD81 support TGF- β 1 signaling in EWI-2-depleted cells (Figure 7A and 7B), it is likely that CD9 (and CD81) is required for the enhanced invasion and diminished proliferation seen in EWI-2-depleted cells. Indeed, upon removal of CD9 from SK-Mel-28 cells, EWI-2 knockdown had markedly lost the stimulatory effect on invasion (Figure 7C) and no longer significantly inhibited proliferation (Figure 7D). CD81 knockdown also substantially eliminated the facilitating effect of EWI-2 depletion on invasion (Figure 7C). As a negative control, knockdown of CD151 had minimal effect on cell invasion (Figure 7C) or cell proliferation (Figure 7D).

Discussion

As melanocytes become malignant and then metastatic, TGF- β signaling experiences a “present-absent-pres-

ent” oscillation [4-6]. However, mechanisms underlying the regulation of melanoma sensitivity to TGF- β have remained elusive. Here we show that EWI-2, a novel negative regulator of TGF- β signaling, plays a major role during melanoma progression. EWI-2 is absent in melanocytes, where cytostatic TGF- β effects are pronounced. EWI-2 is then upregulated in melanoma cells, where it negatively regulates TGF- β signaling, thereby reversing the cytostatic effects and allowing for cell proliferation and survival. Subsequent loss of EWI-2 then enables a new phase of TGF- β signaling, leading to enhanced melanoma invasion and metastasis. Although specific mechanisms responsible for changes in EWI-2 expression remain to be identified, we have made substantial progress in understanding the consequences of altered EWI-2 expression.

EWI-2 negatively regulates TGF- β 1 signaling

Ingenuity pathway analysis (IPA) of microarray results produced an unbiased list of upstream regulatory proteins potentially responsible for changes in gene expression caused by EWI-2 depletion. Near the top of this list was TGF- β 1, a signaling molecule that inhibits primary melanoma cell growth, but stimulates invasion and metastasis [4, 6]. In experiments involving manipulation of EWI-2 expression and TGF- β signaling in multiple melanoma cell lines, we confirmed that TGF- β signaling is negatively regulated by EWI-2. Consistent with this, p-Smad2/3 level was significantly elevated *in vivo* in xenograft tumors lacking EWI-2, and in human tumors with lower EWI-2 levels. Furthermore, inhibition of TGF- β 1 signaling by T β R1 inhibitor SB-431542 [30], or by Smad2 knockdown, essentially eliminated the effect of EWI-2 knockdown on (i) cell proliferation, (ii) cell invasion, and (iii) expression of protein biomarkers associated with proliferation, EMT and metastasis/invasion. Taken together, these results firmly demonstrate that EWI-2 negatively regulates the TGF- β pathway.

EWI-2 supports melanoma tumor growth

We established that EWI-2 protein is absent in melanocytes, but its level is significantly elevated in human malignant melanoma samples. This result is consistent with EWI-2 mRNA being preferentially elevated in cell lines derived from human melanoma, compared to other cancers [23] (also see Oncomine database). We also used multiple melanoma cell lines as well as MSTCs to demonstrate that EWI-2 supports melanoma cell proliferation and growth *in vivo* and/or *in vitro*. Upon depletion of EWI-2 using multiple siRNAs or shRNAs, melanoma cells showed impaired primary tumor growth *in vivo*, diminished lung colony size *in vivo*, reduced cell growth

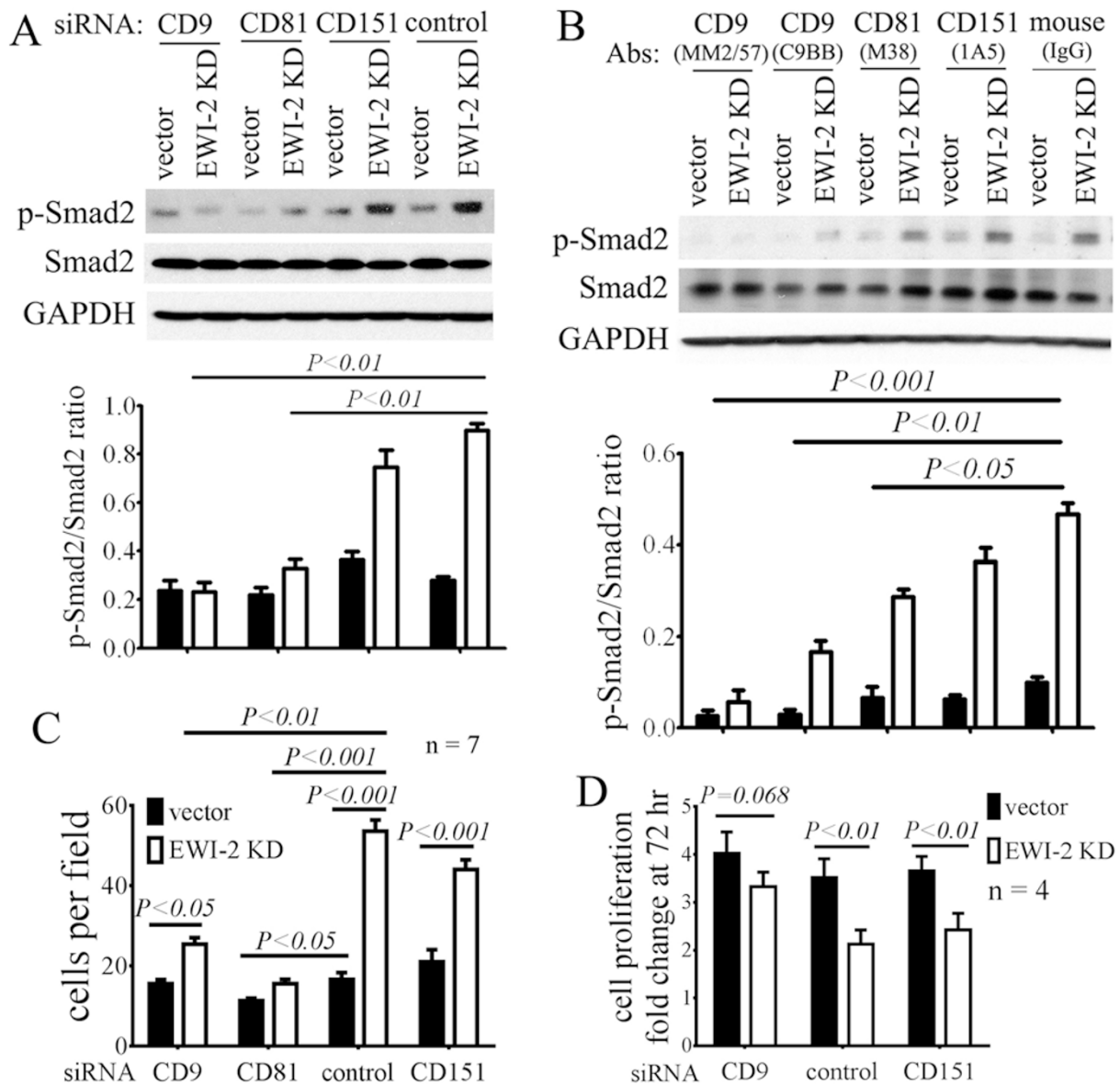


Figure 7 Functions upregulated due to EWI-2 depletion are dependent on CD9 and CD81. **(A)** Effects of tetraspanin protein knockdown on p-Smad2 levels. After siRNA treatment for 72 h, cells were incubated with latent TGF- β 1 (20 ng/ml; 30 min), prior to lysis in 1% Trion-X 100 for western blot analysis. Quantitation is shown in the lower panel ($n = 4$). **(B)** Antibody blocking effects on Smad2 phosphorylation. Cells were starved for 6 h and treated with 5 μ g/ml antibodies in serum-free medium for 45 min, and then incubated with 20 ng/ml latent TGF- β 1 for 30 min, prior to lysis in 1% Trion-X 100 for western blot analysis. Quantitation is shown in the lower panel ($n = 3$). **(C)** Effects of EWI-2 knockdown on cell invasion following knockdown of CD9, CD81, and CD151. SK-Mel-28 cells, with or without EWI-2 depletion, were treated with CD9, CD81, or CD151 siRNA for 72 h, and then tested for cell invasion. **(D)** SK-Mel-28 cells, with or without EWI-2 depletion, were treated with CD9 or CD151 siRNA for 72 h, and then the cells were counted.

in vitro, and substantially enhanced cell cycle arrest at G0/G1 phases, with corresponding changes in expression of 4 key cell cycle regulatory proteins. These findings indicate that EWI-2 supports melanoma growth by supporting cell cycle progression, which is consistent with its negative regulation of cytostatic effects of TGF- β .

EWI-2 and melanoma metastasis

Several results showed here support that EWI-2/IgSF8 acts as a negative regulator of melanoma metastasis. First, EWI-2 protein expression was downregulated in metastatic patient samples, relative to human primary melanoma samples. Second, depletion of EWI-2 from

both human and mouse melanoma cell lines significantly increased metastasis to mouse lungs. Third, knockdown of EWI-2 markedly increased cell migration and invasion in multiple melanoma cell lines, while triggering substantial cell elongation. Fourth, EWI-2 expression levels inversely correlated with invasion potentials of MSTCs. Confirming a causal link between EWI-2 and invasion, overexpression of EWI-2 in highly invasive MSTCs (with low endogenous EWI-2 expression) markedly inhibited invasion.

EMT typically accompanies increased invasion, migration and metastasis in cancer cells [37]. Although melanocytes are non-epithelial, accumulating evidence shows that melanoma cells undergo pseudo-EMT changes [6]. We observed molecular changes (loss of E-cadherin and β -catenin and gain of vimentin expression) and morphological changes (decreased cell-cell adhesion) consistent with pseudo-EMT [38]. Loss of cell-cell adhesion facilitates a single-cell mode of motility that can be more conducive to tumor cell metastasis [39]. In addition, cell elongation due to EWI-2 depletion may facilitate invasion and metastasis, by an ‘elongated mesenchymal’ mode of movement [40]. Notably, β -catenin may suppress melanoma invasion by a mechanism that prevents cell elongation [41], thus consistent with our observations of decreased β -catenin expression, increased elongation and increased invasion in EWI-2-depleted cells.

As seen from TGF- β receptor inhibitor experiments (using SB-431542) and from Smad2 knockdown experiments, EWI-2 suppression of invasion/metastasis is almost entirely due to inhibition of TGF- β signaling. Of particular importance is SB-431542 inhibition of TGF- β -dependent CD271/NGFR expression. CD271 has attracted attention as a melanoma-initiating cell marker, and its expression correlates with higher metastatic potential [33, 34]. Here we show that CD271 expression level is markedly increased in EWI-2-depleted cells through a TGF- β 1-dependent mechanism (enhanced by exogenous TGF- β 1 treatment; diminished by TGF- β 1 inhibition). Moreover, depletion of CD271 substantially reversed the increase in cell invasion seen in EWI-2-depleted cells. These data suggest that CD271 plays a major role in TGF- β 1-dependent melanoma cell invasion that is induced by EWI-2 depletion. Because CD271 may support melanoma stem cell-like functions [33, 34], and EWI-2 diminishes the expression level of CD271, we speculate that EWI-2 may inhibit melanoma stem cell-like functions, which remains to be tested.

How does EWI-2 inhibit TGF- β 1 signaling

When EWI-2 is absent, tetraspanin proteins CD9 and

CD81 make critical contributions to enhanced T β R2-T β R1 receptor complex formation, leading to elevated TGF- β signaling (Figure 8B). This conclusion is supported by CD9 and CD81 knockdown and mAb inhibition results. Our data also show that cell surface CD9 undergoes a substantial reorganization (towards homo-oligomers), and can associate with T β R2 with support from CD81. Thus, CD9 and CD81 appear to be well positioned to enhance T β R2-T β R1 receptor complex formation, leading to elevated TGF- β 1 signaling. In addition, CD9 and/or CD81 are abundantly expressed in nearly all MSTCs that we analyzed (Supplementary information, Figure S1B), and in the majority of primary and metastatic melanoma samples analyzed elsewhere (see Geodataset GDS3966). CD9 and CD81 were not previously known to support TGF- β 1 signaling, likely due to the sequestering effect of EWI-2.

When EWI-2 is present, it associates directly with tetraspanin proteins CD9 and CD81 [7-9], and CD9 is less able to form homo-oligomers [11] as confirmed here in melanoma cells. Consequently CD9 (and probably also CD81) becomes less available to support T β R2-T β R1 association (Figure 8A), leading to decreased TGF- β 1 signaling, diminished invasion and metastasis, and decreased cytostasis (i.e., elevated proliferation). CD9 and CD81 may also associate with several other partner proteins (e.g., claudin-1, CD44, MHC class I, CD224 and EpCAM) [42, 43], but these interactions may not be of sufficient proximity and stoichiometry to mimic the sequestering effect of EWI-2.

In EWI-2-depleted cells, both CD9 and CD81 are required for the enhanced TGF- β signaling that supports elevated melanoma migration and invasion. CD9 is also needed for TGF- β -dependent inhibition of melanoma proliferation. The requirement for CD81 to support inhibition of proliferation in EWI-2-depleted cells was less obvious. We speculate that CD81 knockdown (but not CD9 knockdown) might create an additional unknown deficiency in EWI-2-depleted cells, such that proliferation is not restored even though the inhibitory effect of EWI-2 on TGF- β signaling is diminished. In conclusion, functions resulting from EWI-2 depletion (i.e., upregulated TGF- β signaling, increased invasion/metastasis, and diminished proliferation) are almost entirely dependent on contributions of CD9, and to a lesser extent CD81.

CD9 overexpressed in melanoma cells may inhibit anchorage-independent cell growth and support invasion [12]. On the other hand, CD9 is also suggested to suppress melanoma metastasis [44]. We speculate that variations in levels of EWI-2 could at least partly explain these discrepancies in the actions of CD9. In several other cancer cell types CD9 and CD81 have been linked

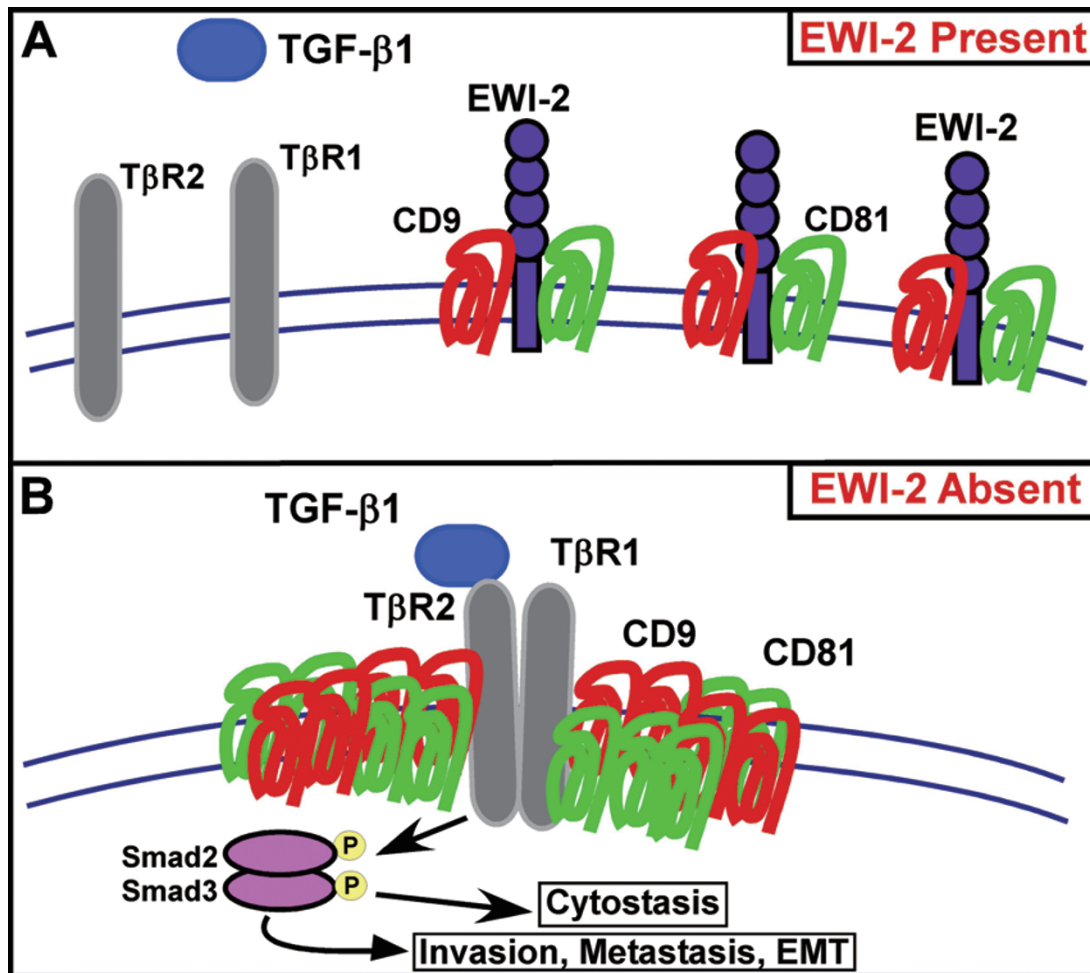


Figure 8 Schematic diagram showing effects of EWI-2 depletion. **(A)** When EWI-2 is present, tetraspanin proteins CD9 and CD81 are sequestered into hetero-oligomer complexes with EWI-2. Hence, CD9 and CD81 are unavailable to assist with T β R1-T β R2 association. **(B)** In the absence of EWI-2, more CD9 homo-oligomers are present and assisted by CD81; they aid in the association of T β R1 with T β R2. Consequently, TGF- β 1 signaling is upregulated, leading to Smad2 activation, inhibition of cell proliferation, and stimulation of melanoma invasion and metastasis.

to cell proliferation [45, 46] and CD9 can have tumor suppressor-like properties [47, 48]. However, potential roles for EWI-2 and TGF- β were not considered in those studies.

Additional implications

Because TGF- β signaling makes major contributions to melanoma progression and metastasis, strategies are being developed for therapeutic intervention, with a particular focus on various TGF- β isoforms and receptor proteins (T β R1, T β R2 and T β R3) [6]. We suggest that for EWI-2-deficient patients, targeting CD9 and CD81 should impair TGF- β signaling, leading to reduced melanoma metastasis. In this regard, we already show here that anti-CD9 and anti-CD81 antibodies markedly di-

minished TGF- β signaling as evidenced by a decrease in p-Smad2 levels in melanoma cells, and elsewhere that an anti-CD9 mAb inhibited melanoma transendothelial migration [13]. Another approach would be to prevent the loss of EWI-2 expression in metastatic melanoma cells, thereby sequestering both CD9 and CD81 and limiting their pro-metastatic, pro-TGF- β contributions.

It is not yet known whether functions of CD9 and CD81 in other cell types might also be affected by EWI-2 expression, and/or involve regulation of TGF- β signaling. For example, EWI-2 and/or TGF- β inhibition could conceivably modulate CD9-dependent suppression of metastasis in other tumor cell types [48], and/or CD9 and CD81 contributions to sperm-egg fusion [49]. Also we speculate that EWI-2 effects on HCV infection [19]

and oocyte fertilization [20] might involve regulation of TGF- β 1 signaling, which remains to be tested.

Why does EWI-2 support primary melanoma growth in this study, but suppress glioblastoma growth in a previous study [18]? Possibly, orthotopic glioblastoma xenograft growth (compared to melanoma) may be more dependent on invasion, which would be inhibited by EWI-2. Indeed, EWI-2 did not inhibit proliferation of cultured glioblastoma cells, but it did inhibit their migration and invasion [18]. It remains to be determined whether EWI-2-dependent inhibition of TGF- β 1 signaling may underlie the effects of EWI-2 in glioblastoma.

In conclusion, our results demonstrate (i) a novel positive regulation of TGF- β 1 signaling by CD9 and CD81 and (ii) a novel negative regulation of TGF- β 1 signaling by EWI-2, which prevents CD9 and CD81 from assisting in T β R2-T β R1 complex formation. These findings may have relevance not only to melanoma, but also to TGF- β contributions to the progression of other cancer types, cancer stem cell propagation, immune suppression, and fibrosis in lungs and other organs [28].

Materials and Methods

Cell culture, antibodies, and other reagents

Human (SK-Mel-28, SK-Mel-5 and 501mel) and mouse (B16F10) melanoma cell lines were from American Type Culture Collection (ATCC, Manassas, VA, USA) and cultured in DMEM with 10% FBS (Sigma, MO, USA) and 1% penicillin-streptomycin (Invitrogen, Grand Island, NY, USA). A panel of MSTCs, isolated directly from human patient samples, was provided by Dr Levi Garraway [21]. MSTCs were cultivated in DMEM with 10% FBS and 1% penicillin-streptomycin. Antibodies to EWI-2, CD9 (C9BB), CD81 (M38) and CD151 (5C11, 1A5) were referenced elsewhere [10]. Anti-EWI-F (MX1) was prepared against recombinant soluble protein in our laboratory. Antibodies to CD9 (MM2/57), β -catenin, glyceraldehyde-3-phosphate dehydrogenase (GAPDH) and β -actin were from EMD Millipore (Billerica, MA, USA). Antibodies to p-Smad2 (Ser465/467), p-Smad2 (Ser465/467)/Smad3 (Ser423/425; D27F4), CDK4 (DCS156), and T β R2 (D3A1) were from Cell Signaling Technology (Danvers, MA, USA). T β R1 (MM0015-8G33) antibody was from Abcam (Cambridge, MA, USA). Antibodies to cyclin E, cyclin D1, pSmad2/3 (Ser423/425) and Smad2 were from Santa Cruz Biotechnology, Inc. (Santa Cruz, CA, USA). Anti-E-cadherin was from BD Biosciences (San Jose, CA, USA) and anti-CD271 was from BioLegend (San Diego, CA, USA). Anti-mouse IGSF8/EWI-2 antibody was from R&D Systems (Minneapolis, MN, USA). TGF- β antibody was from Pierce Biotechnology (Thermo Scientific, Rockford, IL, USA).

shRNAs: human EWI-2 (RHS4533-EG93185, RHS4531-EG93185), mouse EWI-2 (RMM4534-EG140559), and EWI-F (RHS4531-EG5738) plasmid sets were from Open Biosystems (Lafayette, CO, USA) and pLKO.1 puro vector plasmid (Catalog No. 8453) was from Addgene (Cambridge, MA, USA).

siRNAs: ON-TARGETplus for human IGSF8 siRNA set (J-

015148), ON-TARGETplus for human NGFR (CD271) siRNA set (J-009340), siGENOME human CD9 siRNA (D-017252-04), siGENOME human CD81 siRNA (D-017257-05), and siGENOME human CD151 siRNA (D-003637-04) were from Dharmacon, Inc. (Chicago, IL, USA). Human validated Smad2 siRNA (VHS41107) was from Invitrogen.

T β R1 kinase inhibitor SB-431542 was from EMD Millipore. Human latent TGF- β 1 and active TGF- β 1 were from Cell Signaling Technology.

Immunohistochemistry

Human melanoma tissue microarray slides (ME1002, ME1004a, and ME2082a, duplicate for each) were from US Biomax Inc. (Rockville, MD, USA). Three microarray slides, including samples from 229 malignant primary melanomas, 84 metastatic malignant melanomas, 24 benign nevi, and 21 normal skin tissues, were immunostained for EWI-2 using Alkaline Phosphatase Immunohistochemistry Detection Kit (ZYAGEN, San Diego, CA, USA). One slide (ME1004a, including 56 malignant primary melanomas, 20 metastatic malignant melanomas and 24 benign nevi) was used for p-Smad2/3 staining. Slides were deparaffinized and rehydrated, then boiled in 10 mmol/L citrate buffer (pH 6.0) for 15 min, and blocked with serum for 1 h. Slides were incubated with anti-EWI-2 (5 μ g/ml; 4 $^{\circ}$ C, overnight) or anti-p-Smad2/3 (Santa Cruz Technology, 1:2 000 dilution; 4 $^{\circ}$ C, overnight), and then with biotinylated secondary antibody (1 h) and streptavidin-alkaline phosphatase (AP) conjugate (30 min). After color development (Fast Red solution) and hematoxylin counterstaining, results were analyzed by light microscopy and scored by a dermatopathology expert. Relative staining intensity and fraction of tumor area were each graded (score 0-3) and results were multiplied (to give total score 0-9).

Stable and transient knockdown

For stable knockdown, lentiviral plasmids containing EWI-2 or EWI-F shRNAs were purified and transfected together with pCMV-dR8.91 and VSV-G plasmids into HEK293T cells (ATCC) using lipofectamineTM 2000. Medium containing lentivirus was collected 48 h and 72 h after transfection and used to infect target cells for 12 h. Stable cells were selected with 5 μ g/ml puromycin (Invitrogen). For transient knockdown, 20 nM siRNAs were reversely transfected into 1.5×10^5 cells into 6-well plates using lipofectamineTM RNAiMAX (Invitrogen). Transfection medium was replaced (at 12 h) and siRNA efficiency was examined at 72 h by western blotting.

In vivo tumor growth and lung metastasis assays

For *in vivo* tumor growth, SK-Mel-28 cells (1.0×10^6 or 5.0×10^5) were injected s.c. into both flanks of nude mice. Every 5-7 days tumor sizes were measured by calipers. If tumor size reached 2 cm, mice were sacrificed. At the end of each experiment, tumors were excised and weighed. For lung metastasis experiments, SK-Mel-28 (2.0×10^6) and B16F10 (2.0×10^5) were injected i.v. into SCID Beige mice and C57BL/6 mice, respectively. To visualize SK-Mel-28 colonies, mice were killed at 6 weeks, 15% India ink was immediately injected into lung through trachea, and then lungs were isolated and fixed in Fekete's solution. Lungs containing B16F10 colonies were isolated and fixed in Bouin's solution. Lungs colonies were counted under light microscope.

Migration, invasion and cell aggregation assays

Serum-starved cells (5.0×10^4) were added in duplicate to Boyden chambers with polycarbonate membranes (8 μ m pore size, 6.5-mm diameter; Transwell, Corning Life Sciences, Acton, MA, USA) or to Matrigel invasion chambers with polyethylene terephthalate membrane (8 μ m pore size, BD Biosciences). After overnight migration/invasion towards media containing 10% FBS, cells on top membrane were removed using a cotton swab, while cells on the lower membrane were fixed with methanol and stained with Giemsa solution (Sigma). Ten fields per well were photographed randomly under light microscopy and mean cell number in each field was calculated for each of 3-4 replicates. To assess cell aggregation, newly trypsinized cells (1.0×10^4) in 50 μ l of culture media were suspended in hanging drops for 3 h in a humid 5% CO₂ incubator at 37 °C. After pipetting 10 times through a 200 μ l tip, cells were counted to yield aggregated number/total cell number.

Cell proliferation and cell cycle assays

Proliferation was assessed using an Automated Cell Counter (Invitrogen) at defined intervals after plating. For cell cycle analysis, cells were fixed (in cold 70% ethanol; 2 h; 4 °C), washed in PBS, then stained with Propidium Iodide (PI, Roche Applied Science, Indianapolis, IN, USA) solution (50 mg/ml PI, 10 mg/ml RNase A (Invitrogen), 0.05% Triton-X-100) for 45 min at 4 °C in the dark. Cell cycle results were analyzed by flow cytometry (BD FACSCalibur, Franklin Lakes, NJ, USA) and processed using FlowJo software (Ashland, OR, USA).

DNA microarray

Total RNA from SK-Mel-28 transfected cells (expressing EWI-2 shRNA or control shRNA) was extracted using the RNeasy Mini Kit (QIAGEN, Valencia, CA). RNA (1 μ g) was analyzed in two replicates using the U133A 2.0 Affymetrix gene chip array (at the Dana-Farber Cancer Institute Microarray Core Facility). Microarray data were processed using dChip software and analyzed using the IPA software 'Core analysis' function (www.ingenuity.com). The GenePattern [50] 'Multiplot' module was used to produce the volcano plot.

Immunoprecipitation and immunoblotting

Intact SK-Mel-28 cells were biotinylated, lysed in 1% Brij 99 or Brij 96, and then immunoprecipitation and immunoblotting were carried out as described [11].

Immunofluorescence

Cells grown on glass coverslips were treated with 50 ng/ml latent TGF- β 1, 10 μ M SB-431542 or the same volume of DMSO for 30 min, and then fixed with 4% paraformaldehyde at 4 °C for 15 min and permeabilized by 0.1% Triton X-100 in PBS for 5 min. Cells were then blocked with 3% BSA in PBS (w/v), immunolabeled with p-Smad2/3 primary antibody (D27F4 from Cell Signaling Technology, 1:200 dilution) for 1 h, followed by Alexa Fluor 488-conjugated goat anti-rabbit IgG for 1 h. Coverslips were mounted with ProLong Gold antifade mounting media containing DAPI and imaged using a Leica SP5X laser scanning confocal microscope (Leica Microsystems, Chicago, IL, USA).

Acknowledgments

This work was supported by the National Institutes of Health (CA42368 to MEH).

References

- 1 Flaherty KT. Targeting metastatic melanoma. *Annu Rev Med* 2012; **63**:171-183.
- 2 Tsao H, Chin L, Garraway LA, Fisher DE. Melanoma: from mutations to medicine. *Genes Dev* 2012; **26**:1131-1155.
- 3 Tuong W, Cheng LS, Armstrong AW. Melanoma: epidemiology, diagnosis, treatment, and outcomes. *Dermatol Clin* 2012; **30**:113-124, ix.
- 4 Javelaud D, Alexaki VI, Mauviel A. Transforming growth factor-beta in cutaneous melanoma. *Pigment Cell Melanoma Res* 2008; **21**:123-132.
- 5 Lasfar A, Cohen-Solal KA. Resistance to transforming growth factor beta-mediated tumor suppression in melanoma: are multiple mechanisms in place? *Carcinogenesis* 2010; **31**:1710-1717.
- 6 Perrot CY, Javelaud D, Mauviel A. Insights into the transforming growth factor-beta signaling pathway in cutaneous melanoma. *Ann Dermatol* 2013; **25**:135-144.
- 7 Stipp CS, Kolesnikova TV, Hemler ME. EWI-2 is a major CD9 and CD81 partner, and member of a novel Ig protein subfamily. *J Biol Chem* 2001; **276**:40545-40554.
- 8 Charrin S, Le Naour F, Labas V, et al. EWI-2 is a new component of the tetraspanin web in hepatocytes and lymphoid cells. *Biochem J* 2003; **373**(Part 2):409-421.
- 9 Clark KL, Zeng Z, Langford AL, Bowen SM, Todd SC. Pgrl is a major CD81-associated protein on lymphocytes and distinguishes a new family of cell surface proteins. *J Immunol* 2001; **167**:5115-5121.
- 10 Kolesnikova TV, Stipp CS, Rao RM, Lane WS, Luscinskas FW, Hemler ME. EWI-2 modulates lymphocyte integrin alpha4beta1 functions. *Blood* 2004; **103**:3013-3019.
- 11 Yang XH, Kovalenko OV, Kolesnikova TV, et al. Contrasting Effects of EWI proteins, integrins, and protein palmitoylation on cell surface CD9 organization. *J Biol Chem* 2006; **281**:12976-12985.
- 12 Fan J, Zhu GZ, Niles RM. Expression and function of CD9 in melanoma cells. *Mol Carcinog* 2010; **49**:85-93.
- 13 Longo N, Yanez-Mo M, Mittelbrunn M, et al. Regulatory role of tetraspanin CD9 in tumor-endothelial cell interaction during transendothelial invasion of melanoma cells. *Blood* 2001; **98**:3717-3726.
- 14 Hong IK, Byun HJ, Lee J, et al. The tetraspanin CD81 protein increases melanoma cell motility by up-regulating metalloproteinase MT1-MMP expression through the pro-oncogenic Akt-dependent Sp1 activation signaling pathways. *J Biol Chem* 2014; **289**:15691-15704.
- 15 Mischiati C, Natali PG, Sereni A, et al. cDNA-array profiling of melanomas and paired melanocyte cultures. *J Cell Physiol* 2006; **207**:697-705.
- 16 Si Z, Hersey P. Expression of the neuroendocrine antigen and analogues in melanoma. CD9 expression appears inversely related to metastatic potential of melanoma. *Int J Cancer* 1993; **54**:37-43.
- 17 Stipp CS, Kolesnikova TV, Hemler ME. EWI-2 regulates α 3 β 1 integrin-dependent cell functions on laminin-5. *J Cell*

- Biol* 2003; **163**:1167-1177.
- 18 Kolesnikova TV, Kazarov AR, Lemieux ME, *et al.* Glioblastoma inhibition by cell surface immunoglobulin protein EWI-2, *in vitro* and *in vivo*. *Neoplasia* 2009; **11**:77-86.
 - 19 Rocha-Perugini V, Montpellier C, Delgrange D, *et al.* The CD81 partner EWI-2wint inhibits hepatitis C virus entry. *PLoS One* 2008; **3**:e1866.
 - 20 Glazar AI, Evans JP. Immunoglobulin superfamily member IgSF8 (EWI-2) and CD9 in fertilisation: evidence of distinct functions for CD9 and a CD9-associated protein in mammalian sperm-egg interaction. *Reprod Fertil Dev* 2009; **21**:293-303.
 - 21 Lin WM, Baker AC, Beroukhim R, *et al.* Modeling genomic diversity and tumor dependency in malignant melanoma. *Cancer Res* 2008; **68**:664-673.
 - 22 Jakowlew SB. Transforming growth factor-beta in cancer and metastasis. *Cancer Metastasis Rev* 2006; **25**:435-457.
 - 23 Scherf U, Ross DT, Waltham M, *et al.* A gene expression database for the molecular pharmacology of cancer. *Nat Genet* 2000; **24**:236-244.
 - 24 Stipp CS, Orlicky D, Hemler ME. FPRP: A major, highly stoichiometric, highly specific CD81 and CD9-associated protein. *J Biol Chem* 2001; **276**:4853-4862.
 - 25 Gaggioli C, Sahai E. Melanoma invasion — current knowledge and future directions. *Pigment Cell Res* 2007; **20**:161-172.
 - 26 Wrighton KH, Lin X, Feng XH. Phospho-control of TGF-beta superfamily signaling. *Cell Res* 2009; **19**:8-20.
 - 27 Lonn P, Moren A, Raja E, Dahl M, Moustakas A. Regulating the stability of TGFbeta receptors and Smads. *Cell Res* 2009; **19**:21-35.
 - 28 Akhurst RJ, Hata A. Targeting the TGFbeta signalling pathway in disease. *Nat Rev Drug Discov* 2012; **11**:790-811.
 - 29 Massague J. TGFbeta signalling in context. *Nat Rev Mol Cell Biol* 2012; **13**:616-630.
 - 30 Laping NJ, Grygielko E, Mathur A, *et al.* Inhibition of transforming growth factor (TGF)-beta1-induced extracellular matrix with a novel inhibitor of the TGF-beta type I receptor kinase activity: SB-431542. *Mol Pharmacol* 2002; **62**:58-64.
 - 31 Huber MA, Kraut N, Beug H. Molecular requirements for epithelial-mesenchymal transition during tumor progression. *Curr Opin Cell Biol* 2005; **17**:548-558.
 - 32 Qiao B, Johnson NW, Gao J. Epithelial-mesenchymal transition in oral squamous cell carcinoma triggered by transforming growth factor-beta1 is Snail family-dependent and correlates with matrix metalloproteinase-2 and -9 expressions. *Int J Oncol* 2010; **37**:663-668.
 - 33 Civenni G, Walter A, Kobert N, *et al.* Human CD271-positive melanoma stem cells associated with metastasis establish tumor heterogeneity and long-term growth. *Cancer Res* 2011; **71**:3098-3109.
 - 34 Boiko AD, Razorenova OV, van de Rijn M, *et al.* Human melanoma-initiating cells express neural crest nerve growth factor receptor CD271. *Nature* 2010; **466**:133-137.
 - 35 Bakin AV, Tomlinson AK, Bhowmick NA, Moses HL, Arteaga CL. Phosphatidylinositol 3-kinase function is required for transforming growth factor beta-mediated epithelial to mesenchymal transition and cell migration. *J Biol Chem* 2000; **275**:36803-36810.
 - 36 Thannickal VJ, Lee DY, White ES, *et al.* Myofibroblast differentiation by transforming growth factor-beta1 is dependent on cell adhesion and integrin signaling via focal adhesion kinase. *J Biol Chem* 2003; **278**:12384-12389.
 - 37 Nguyen DX, Bos PD, Massague J. Metastasis: from dissemination to organ-specific colonization. *Nat Rev Cancer* 2009; **9**:274-284.
 - 38 Schmalhofer O, Brabletz S, Brabletz T. E-cadherin, beta-catenin, and ZEB1 in malignant progression of cancer. *Cancer Metastasis Rev* 2009; **28**:151-166.
 - 39 Giampieri S, Manning C, Hooper S, Jones L, Hill CS, Sahai E. Localized and reversible TGFbeta signalling switches breast cancer cells from cohesive to single cell motility. *Nat Cell Biol* 2009; **11**:1287-1296.
 - 40 Orgaz JL, Sanz-Moreno V. Emerging molecular targets in melanoma invasion and metastasis. *Pigment Cell Melanoma Res* 2013; **26**:39-57.
 - 41 Arozarena I, Bischof H, Gilby D, Belloni B, Dummer R, Wellbrock C. In melanoma, beta-catenin is a suppressor of invasion. *Oncogene* 2011; **30**:4531-4543.
 - 42 Kovalenko OV, Yang XH, Hemler ME. A novel cysteine cross-linking method reveals a direct association between claudin-1 and tetraspanin CD9. *Mol Cell Proteomics* 2007; **6**:1855-1867.
 - 43 Le Naour F, Andre M, Greco C, *et al.* Profiling of the tetraspanin web of human colon cancer cells. *Mol Cell Proteomics* 2006; **5**:845-857.
 - 44 Miyake M, Inufusa H, Adachi M, *et al.* Suppression of pulmonary metastasis using adenovirally motility related protein-1 (MRP-1/CD9) gene delivery. *Oncogene* 2000; **19**:5221-5226.
 - 45 Oren R, Takahashi S, Doss C, Levy R, Levy S. TAPA-1, the target of an antiproliferative antibody, defines a new family of transmembrane proteins. *Mol Cell Biol* 1990; **10**:4007-4015.
 - 46 Inui S, Higashiyama S, Hashimoto K, Higashiyama M, Yoshikawa K, Taniguchi N. Possible role of coexpression of CD9 with membrane-anchored heparin-binding EGF-like growth factor and amphiregulin in cultured human keratinocyte growth. *J Cell Physiol* 1997; **171**:291-298.
 - 47 Romanska HM, Berditchevski F. Tetraspanins in human epithelial malignancies. *J Pathol* 2011; **223**:4-14.
 - 48 Zoller M. Tetraspanins: push and pull in suppressing and promoting metastasis. *Nat Rev Cancer* 2009; **9**:40-55.
 - 49 Rubinstein E, Ziyat A, Wolf JP, Le Naour F, Boucheix C. The molecular players of sperm-egg fusion in mammals. *Semin Cell Dev Biol* 2006; **17**:254-263.
 - 50 Reich M, Liefeld T, Gould J, Lerner J, Tamayo P, Mesirov JP. GenePattern 2.0. *Nat Genet* 2006; **38**:500-501.

(Supplementary information is linked to the online version of the paper on the *Cell Research* website.)